ENVIRONMENTAL DYNAMICS AND ELECTRON TRANSFER REACTIONS

JAMES T. HYNES, EMILY A. CARTER,[a] GIOVANNI CICCOTTI,[b]
HYUNG J. KIM & DOMINIC A. ZICHI [c]
Department of Chemistry and Biochemistry
University of Colorado
Boulder, CO 80309-0215, USA

MAURO FERRARIO
Istituto di Fisica Teorica
Universitá di Messina
Messina, ITALY

RAYMOND KAPRAL
Chemistry Physics Theory Group
Department of Chemistry
University of Toronto
Toronto, Ontario M5S 1A1, CANADA

ABSTRACT. Recent theoretical and computer simulation work on the dynamics associated with electron transfer processes in polar solvents is described. This includes solvent relaxation subsequent to photo-induced charge transfer, adiabatic electron transfer rates, and the solvent influence on the electronic states relevant to electron transfers.

1. INTRODUCTION

A number of key issues that are evidently relevant for electron transfer (ET) dynamics in the photosynthetic reaction center [1] also arise in the superficially remote context of ET in solution, where the environment for the ET event is provided by the solvent. Among these issues are the timescales for solvent relaxation subsequent to photo-induced ET, the role of the solvent dynamics in influencing the ET rate, and the influence of the solvent on the nature of electronic states having charge transfer character. In the following, we briefly summarize some of our recent theoretical and computer simulation results on

a) Permanent Address: Dept. of Chemistry and Biochemistry, Univ. of California, Los Angeles, CA 90024-1569.

b) Permanent address: Dip. di Fisica, Univ. 'La Sapienza', Pl. A. Moro, 2, 00185 Rome, ITALY.

c) Present Address: Agouron Pharmaceuticals, Inc. 11025 North Torrey Pines Road, La Jolla, CA 92037

J. Jortner and B. Pullman (eds.), Perspectives in Photosynthesis, 133–148.

each of these questions for ET in polar solvents. One can hope that, modulo specific details, the central concepts emerging from these solution studies could be useful in the patently more complex photosynthetic arena.

2. TIME DEPENDENT FLUORESCENCE AND SOLVENT RELAXATION

When a charge separation is induced in a solute by absorption of a photon in a Franck-Condon transition, the solvent--which is initially out of equilibrium with the new charge distribution--will ultimately relax to equilibrium with it (Fig. 1). These solvent dynamics can be probed in time dependent fluorescence (TDF) experiments. [2]

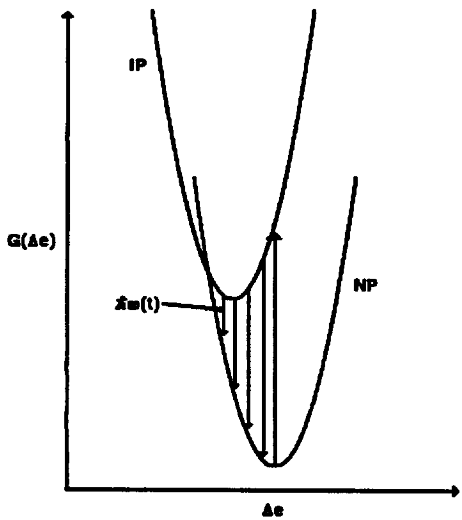

Figure 1. Schematic diagram illustrating time dependent fluorescence transitions of frequency ω(t) between ion pair (IP) and neutral pair (NP) states, versus the numerical value Δe of the solvent coordinate ΔE. See the text.

While earlier work in this area focussed on creating analytic theory and models [3], there has been more recent activity in Molecular Dynamics (MD) computer simulation of the phenomenon [4,5]. Carter and Hynes [5] have studied TDF in a simulation of a neutral pair (NP) DA, photoexcited directly to a charge transfer ion pair (IP) state D^+A^-.

The constituent members of the solute pair (SP) each have mass 40 amu; their centers are rigidly separated by 3.0Å, but the SP is free to translate and rotate. The solvent is composed of 342 rigid dipolar molecules with constituent atoms of mass 40 amu separated from each other by a fixed distance of 2.0Å and with partial charges such that the dipole moment is 2.4D. The number density is $0.012 Å^{-3}$ and the temperature is 250K. This solvent [6], which is very roughly similar to methyl chloride, is akin to members of the class of dipolar aprotic solvents currently under experimental investigation [2].

The total potential energy consists of Lennard-Jones and Coulomb potentials between each atomic site. The LJ parameters are ε/k_B = 200K and σ = 3.5Å for each site in the SP and the solvent.

The solvent dynamics were monitored by following the dynamical collective variable ΔE. This is the difference, at fixed solvent configurations, between the SP-solvent interaction potential energy in the IP and NP states, i.e., an energy gap. For the present model, ΔE is just the Coulomb IP-solvent energy. Note that this variable is well-defined even in the absence of the IP, i.e., in the presence of the NP.

Constant temperature [7] MD simulations were carried out in a periodically replicated cubic box with side length 30.52Å. The equations of motion were integrated via the Verlet algorithm [8] with a time step of 10^{-2} ps. The long range forces were treated by the Ewald summation method [9] and the bond constants for the SP and solvent molecules were implemented with the SHAKE algorithm [10].

In the simulations, the solvent was initially equilibrated to the NP. 198 different initial configurations were then selected, the charges were instantly turned on to produce the IP, and then the ensuing dynamics were examined.

One important characteristic of the solvent subsequent to the FC transition is the normalized TDF shift [3-5]

$$S(t) = \frac{\bar{\omega}(t) - \bar{\omega}(\infty)}{\bar{\omega}(0) - \bar{\omega}(\infty)} = \frac{\Delta\bar{E}(t) - \Delta\bar{E}(\infty)}{\Delta\bar{E}(0) - \Delta\bar{E}(\infty)} , \tag{1}$$

which is related to the average in the nonequilibrium ensemble of the TDF frequency ω and ΔE initially, at time t, and at "infinite" time t=∞, when relaxation has concluded. Figure 2 shows that the relaxation is extensive and rapid, with a distinctly bimodal character. The celerity of the initial relaxation is especially to be noted.

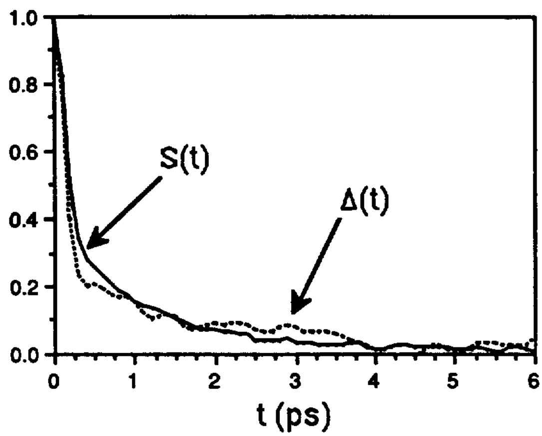

Figure 2. MD results [5] for the TDF shift S(t), Eq. 1. The time correlation function $\Delta(t)$, Eq. 3, is also shown. The absolute magnitude of the shift $\Delta\bar{E}(0) - \Delta\bar{E}(\infty)$ is approximately 1.9×10^3 cm^{-1}

Carter and Hynes expressed the nonequilibrium average $\Delta\bar{E}(t)$--whose dynamics occur in the presence of the IP, but with initial conditions in the solvent determined by the NP--as the average [5]

$$\Delta\bar{E} = \left\langle e^{\beta\Delta E}\right\rangle_{IP}^{-1} \left\langle e^{\beta\Delta E}\,\Delta E(t)\right\rangle_{IP} \tag{2}$$

over an equilibrium IP ensemble. Here $\beta^{-1} = k_B T$. When developed to second order in ΔE, this leads to [5]

$$S(t) \;=\; \left\langle(\delta\Delta E)^2\right\rangle_{IP}^{-1} \left\langle\delta\Delta E\;\delta\Delta E(t)\right\rangle_{IP} \equiv \;\; \Delta(t) \qquad , \tag{3}$$

i.e., an equilibrium time correlation function of the type considered in a number of studies [3-5]. Here $\delta\Delta E = \Delta E - \langle\Delta E\rangle_{IP}$.

Figure 2 shows that this approximation is fairly accurate, so that, in the main, the non-equilibrium average TDF shift can in fact and somewhat remarkably be understood via the dynamics of solvent fluctuations at equilibrium; this was a key assumption of analytic approaches to TDF [3]. (This statement is not true for other measures of the TDF spectrum, the spectral width in particular [5].)

This being the case, further examination of the correlation function $\Delta(t)$ is in order. The most convenient formalism for this purpose is via a rigorous generalized Langevin equation (GLE) for ΔE developed by Zichi *et al.* [11], according to which $\Delta(t)$ satisfies

$$\ddot{\Delta}(t) \;=\; -\omega^2\Delta(t) - \int_0^t d\tau\,\zeta(t-\tau)\dot{\Delta}(\tau) \quad . \tag{4}$$

Here $\omega^2 = \langle(\delta\Delta E)^2\rangle_{IP}^{-1}\,\langle(\delta\dot{\Delta E})^2\rangle_{IP}$ is [12] the square well frequency for the free energy well for fluctuations in ΔE in the presence of the IP. (It was established previously [12) that this well is indeed harmonic.) The time dependent friction coefficient $\zeta(t)$ is essentially the correlation function of the fluctuating generalized force acting on ΔE [11]. It accounts for dissipative ΔE motion associated with the presumably complex solvent dipole librations, reorientations and translations. It can be extracted from the MD-generated $\Delta(t)$ via Fourier transform inversion techniques [11] and is displayed in Fig. 3.

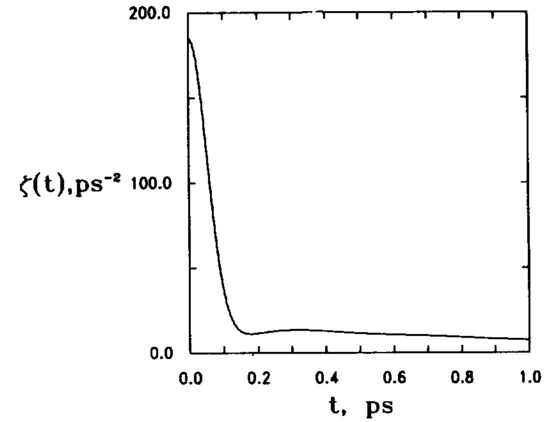

Figure 3. The time dependent friction coefficient $\zeta(t)$ for the ion pair [11].

The substantial initial rapid drop in both the TDF shift S(t) and the tcf $\Delta(t)$ is governed [5] by the frequency ω according to the simple Gaussian behavior $\Delta^G(t) = \exp(-\omega^2 t^2/2)$, as shown in Fig. 4. This is an important observation, since ω^2 is an equilibrium quantity and one can hope to understand it in terms of the electrostatic forces and torques exerted by the solvent on the ion pair via the methods of modern equilibrium statistical mechanics. It can be further shown [11] that the longer time tails of S(t) and $\Delta(t)$ arise from the time dependent friction $\zeta(t)$ and thus contains information on dissipative solvent processes. Just what those processes are and how they can be approximately described analytically remain to be determined. But it is certainly clear from the present results that the popular continuum dielectric model--which would predict an exponential behavior for S(t) and $\Delta(t)$ [3]--fails significantly, a failure recently observed experimentally in femtosecond laser experiments [2]. Figure 4 shows the failure of the exponential decay predicted by a Langevin Equation (LE) simplification of the GLE, in which the time dependence of $\zeta(t)$ is approximated by a delta function. Obviously, a new initiative is required here to generate a useful molecular level description of the solvent dynamics observed in these simulations.

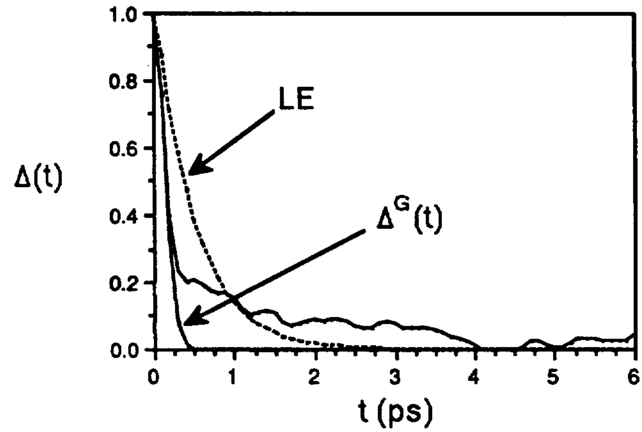

Figure 4. The solvent time correlation function $\Delta(t)$ compared to the Gaussian description $\Delta^G(t)$ and a Langevin equation description [5]. $\Delta(t)$ is called $C(t)$ in many studies.

3. ET REACTION RATES

The possible role of solvent dynamics in influencing charge transfer reaction rates in solution has received considerable recent scrutiny [3]. One particular focus has been the importance of solvent dynamics for electron transfer reaction rate constants k. In the standard Marcus Theory [14], which is a Transition State Theory (TST), the rate constant depends upon solvent free energetics but not upon the solvent dynamics. Recently, there has been an explosive analytical theoretical effort attempting to describe the influence of solvent dynamics in causing departures from the Marcus Theory predictions for k [15-17]. Parallel experimental efforts have indicated that some role is indeed played by the dynamics of the solvent in influencing e transfer rates [18]. Despite these intensive efforts, the picture nonetheless remains somewhat clouded; e.g., measures of solvent free energetics and dynamics employed in the theory and interpretations rely on continuum dielectric theory predictions of uncertain validity.

In response, Zichi, Ciccotti, Ferrario and Hynes (ZCFH) have undertaken [19] MD simulations for a well-defined homogeneous activated ET reaction in which deviations from the Marcus TST Theory due to solvent dynamical effects were examined and quantified [20].

ZCFH have considered the (artificial) model ET reaction

$$A^{-1/2}B^{1/2} \longrightarrow A^{1/2}B^{-1/2} \quad , \tag{5}$$

for a solute pair AB, with A = B, immersed in the solvent described in Sec. 2 (the rationale for the choice of fractional charges is given below). The reactant (R) and product (P) solute pair members with a fixed AB separation of 3Å interact via Coulomb and Lennard-Jones (LJ) potentials with the solvent.

The reaction coordinate adopted was the many-body solvent variable[21]

$$\Delta E = H_R - H_P = V_R^{coul} - V_P^{coul} \quad ; \tag{6}$$

this energy gap is the difference, at fixed solvent configurations, between the R and P Hamiltonians, i.e., between the Coulomb potential energy of interaction between the solvent molecules and the R and P solute pairs respectively. By symmetry, the reaction transition state is obviously located at $\Delta E = 0$. This simple identification via symmetry considerations, which does not require extensive free energy simulations to establish it, together with the established character of the Ewald method applicable for overall charge-neutral systems, provided the rationale for the choice of the model reaction Eq. 5 for this initial study.

Only the electronically adiabatic limit was considered. Thus, the electronic coupling is sufficiently strong to provide a continuous electronic path between reactants and products (see below). This regime is applicable for many short range electron transfers and it is in this regime that solvent dynamical effects should be most pronounced [17].

The prescription for the adiabatic dynamics was the following. Let H_e formally represent the total system Hamiltonian including the electronic degree of freedom. At fixed solvent molecule configurations, the adiabatic Hamiltonian is determined by a straightforward variational calculation based on the trial two state electronic wave function [21] $\Psi = C_R\Psi_R + C_P\Psi_P$ in which Ψ_R and Ψ_P are the diabatic wave functions describing the R and P electronic distributions and the probability amplitudes C_R and C_P depend parametrically on the solvent configurations. The diabatic system Hamiltonians for the R and P charge distributions are $H_R = \langle\Psi_R \mid H_e \mid \Psi_R\rangle$ and $H_P = \langle\Psi_P \mid H_e \mid \Psi_P\rangle$ respectively. The resulting diagonalization then gives the (lowest) energy system adiabatic Hamiltonian for the solute pair as [19]

$$\begin{aligned} H &= \frac{(H_R + H_P)}{2} - \frac{\left[(\Delta E)^2 + 4V_{el}^2\right]^{1/2}}{2} \quad ; \\ V_{el} &= \frac{2H_{RP} - S(H_R + H_P)}{2(1 - S^2)} \quad . \end{aligned} \tag{7}$$

Here $(H_R + H_P)/2 = H_{NP}$ is just the classical system Hamiltonian for a solute neutral pair. V_{el} is a properly symmetrized electronic coupling, independent of the zero of energy, expressed in terms of the matrix element $H_{RP} = \langle\Psi_R \mid H_e \mid \Psi_P\rangle$ and $S = \langle\Psi_R \mid \Psi_P\rangle$, which is the overlap integral. No attempt was made to calculate Vel *a priori*, but rather it was regarded as an input (constant) parameter for the simulations. Note again that Eq. (7) governs the system dynamics.

In this adiabatic description, the quantum reactant occupation probability $C_R^2 = 1 - C_P^2$,

$$C_R^2(\Delta E) = 4V_{el}^2\left[4V_{el}^2 + \left\{\Delta E + \left[(\Delta E)^2 + 4V_{el}^2\right]^{1/2}\right\}^2\right]^{-1} , \tag{8}$$

goes smoothly from unity to zero as ΔE goes from large negative values to large positive values. It can be directly established from the equations of motion associated with Eq. 7 that the dipolar solvent molecules experience the electric field of the apparent classical charge [19]

$$q(\Delta E) = \left[1 - 2C_R^2(\Delta E)\right](e/2) , \tag{9}$$

on the solute pair member A and $-q(\Delta E)$ on member B. This apparent charge $q(\Delta E)$ proceeds smoothly from $q = -e/2$ at large negative ΔE, through $q = 0$ at $\Delta E = 0$, to $q = e/2$ at large positive ΔE. The adiabatic Hamiltonian Eq. (7) can in fact be written (after some taxing algebra) as [19]

$$H = H_{NP} - V_{el} - \int_0^{\Delta E} d\Delta E \left[q(\Delta E)/e\right] ,$$

whose integral contribution emphasizes the electronically "polarizable" character of the solvent-dependent solute pair charge distribution: the charge distribution is solvent-dependent.

The deviation from the Marcus TST Theory prediction k^{TST} was quantified by the transmission coefficient

$$\kappa = k/k^{TST} . \tag{10}$$

This was calculated [19] by a flux time correlation function [22-25], as in other reaction simulations [13,26,27],based on trajectories sampled from an initial equilibrium distribution at the transition state [24,26], here located by $\Delta E = 0$. ZCFH attain the transition state in the simulation by imposing the coordinate and velocity constraints $\Delta E = 0$ and $\Delta\dot{E} = 0$ in a constant temperature simulation. However, this procedure introduces a distortion in the sampling compared to the desired initial equiibrium ensemble which is restricted to $\Delta E = 0$ but not $\Delta\dot{E} = 0$. But as described in detail by Carter, Ciccotti, Hynes and Kapral [28], this distortion can be analytically corrected for, and the transmission coefficient is given correctly by the formula

$$\kappa = \frac{\left\langle D^{-1/2}\Delta\dot{E}\theta[\Delta E(t)]\right\rangle_c}{\left\langle D^{-1/2}\Delta\dot{E}\theta(\Delta\dot{E})\right\rangle_c} , \tag{11}$$

in which D is [28] the sum over all molecules

$$D = m^{-1}\sum_i \nabla_i' \Delta E \cdot \nabla_i' \Delta E \quad ,$$

where ∇_i' denotes the spatial gradient subject to all bond length constraints, θ is the step function and t is a "plateau" time [22-24]. The average $\langle(...)\rangle_c$ denotes the constrained reaction coordinate or "blue moon" ensemble due to Carter *et al.*[28], in which the initial conditions are prepared as described above and at t = 0, the constaint is released, with an appropriate equilibrium distribution of momenta sampled. We pause to note that this procedure can be straightforwardly applied in even more complex reaction problems, with an arbitrary many body, collective configuration-dependent reaction coordinate.

ZCFH first selected a moderate value of the electronic coupling, $V_{el} = 1$ kcal/mol. While no MD-simulated free energy curves are presented here, the approximate free energy curve displayed in Fig. 5 and described in the caption helps to provide perspective on the MD reaction simulation results. In particular, the barrier is cusped; the barrier frequency $\omega_b \sim 4\omega_R$ is estimated by the formula [19] $\omega_b = \omega_R\ [(2\Delta G^{\ddagger}/V_{el}) - 1]^{1/2}$, with ω_R the R well frequency.

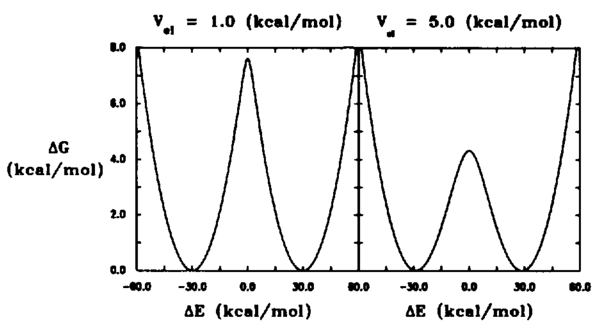

Figure 5. Schematic free energy curves for the two electronic coupling cases. These are generated [19] by a standard macroscopic description[14] with MD-simulated input parameters. See Ref. 19.

A representative example [19] out of 100 trajectories is shown in Fig. 6. There is a direct passage across the transition state, flanked by quite rapid equilibration within the wells. For the very few recrossing trajectories observed, only small excursions off the transition state and single recrossings are involved. The estimated transmission coefficient is $\kappa_{MD} = 0.95 \pm 0.04$. This proximity to unity reflects the feature that recrossings are rare, and Marcus Theory provides an excellent description for this case -- the basic TST assumption (see, e.g., [13]) of no recrossing of the barrier top is well satisfied.

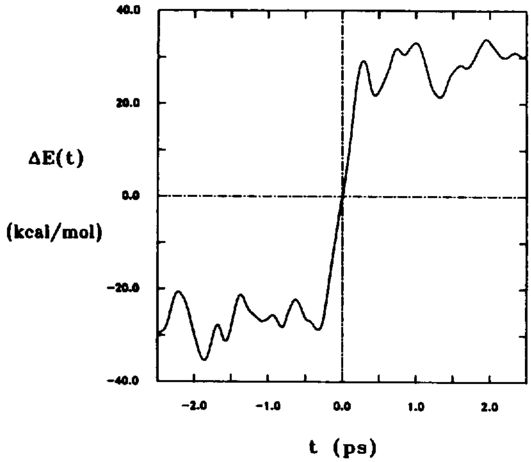

Figure 6. Representative trajectory for the V_{el}=1 kcal/mol case [19].

In the second case studied by ZCFH, the electronic coupling was increased to $V_{el} = 5$ kcal/mol. The estimated barrier (Fig. 5) is somewhat broad: $\omega_b/\omega_R \sim 1.6$. A representative trajectory [19] is displayed in Fig. 7. Recrossing is now pronounced, with repeated recrossings occurring near the barrier top prior to ultimate rapid equilibration in the wells. The estimated transmission coefficient $\kappa_{MD} = 0.59 \pm 0.11$ represents a marked departure from Marcus TST Theory for this case.

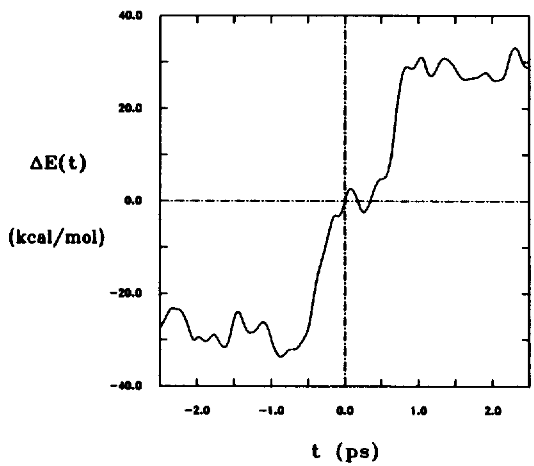

Figure 7. Representative trajectory for the V_{el}=5 kcal/mol case [19].

Most current theories [15-17] for the solvent dynamical influence on κ values for sharp ("cusped") barrier ET reactions derive from the Zusman Theory [15]; this pictures the solvent dynamical effect as arising exclusively from slow overdamped solvent dynamics in the R and P wells and not at the barrier top. It was found that this description does not apply at all to the current simulations [19], essentially due to the vital and dominant importance of the barrier top dynamics.

A theory for activated barrier crossing, which has proved to be strikingly successful for a variety of reaction classes in solution [13,27,29] is Grote-Hynes Theory [17,30], according to which the transmission coefficient is given by the self-consistent relation

$$\kappa_{GH} = \left[\kappa_{GH} + \frac{1}{\omega_b} \int_0^\infty dt\, e^{-\omega_b \kappa_{GH} t} \zeta^\ddagger(t) \right]^{-1} , \qquad (12)$$

where $\zeta^\ddagger(t)$ is the time dependent friction (tdf) for the reaction system at the barrier top. (The GH theory focuses solely on events occurring in the barrier top region.) Evaluation of $\zeta^\ddagger(t)$ requires extensive special simulations at the transition state [13,27,29]. ZCFH followed [19] instead a simpler approximate exploratory route to $\zeta^\ddagger(t)$ and κ_{GH}, now described.

Note that at the transition state $\Delta E=0$, the solute pair charge distribution is that of a neutral pair (NP) (cf. Eq. (8) and Eq. (9)). An estimate of $\zeta^\ddagger(t)$ can then be obtained by determining the actual tdf $\zeta_{NP}(t)$ for a neutral solute pair. This can be determined [11] in precisely the same fashion as described in Sec. 2 for the ion pair friction, and the result is shown in Fig. 8.

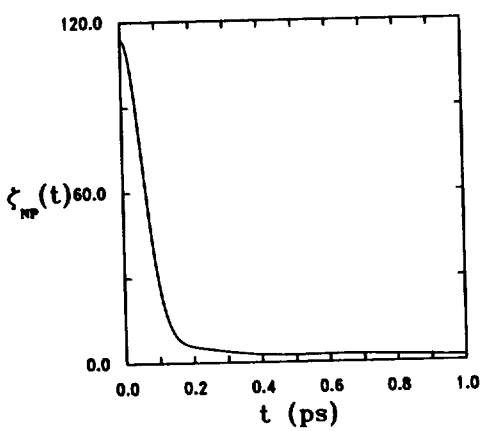

Figure 8. The time dependent friction $\zeta_{NP}(t)$ for a neutral pair [11,19].

This was then used as an approximation for $\zeta^\ddagger(t)$ in the GH Eq. (12), with the results [19] listed in Table 1.

TABLE 1. ET Transmission Coefficients [19]

V_{el}(kcal/mol)	ω_b(ps^{-1})	κ_{MD}	κ_{GH}
1	26.6	0.95±0.04	0.94
5	10.2	0.59±0.11	0.74

The reasonable level of agreement obtained between these approximate κ_{GH} values and κ_{MD} for both the cusped and broad barrier cases examined is very encouraging. It strongly suggests (a) that the barrier region dynamics are the most important aspect of the solvent dynamics (also indicated by the detailed trajectories) and (b) that the shorter time scale solvent dynamics such as those responsible for the rapid decay of $\zeta_{NP}(t)$ in Fig. 8 are those most important in establishing the transmission coefficients and the departure from Marcus TST Theory. These aspects can now be explored for a range of ET reactions in the future.

Finally, the constrained reaction coordinate ensemble (CRCE) [28] provides a prescription for determining rigorous free energy profiles versus ΔE for general ET systems. In particular, the negative gradient $F(\Delta e)$ of the potential of mean force is given by

$$F = \left\langle D^{-1/2} \right\rangle_{c,\Delta e}^{-1} \left\langle D^{-1/2} \frac{\partial \underset{\sim}{r}}{\partial \Delta E} \left[-\frac{\partial}{\partial \underset{\sim}{r}} (V + C) \right] \right\rangle_{c,\Delta e} ,$$

where $\langle (\ldots) \rangle_{c,\Delta e}$ means a CRCE with ΔE equal to the numerical value Δe, $\underset{\sim}{r}$ denotes all coordinates, V is the potential energy and C is a generalized centrifugal potential [28].

4. SOLVA TION AND ELECTRONIC STRUCTURE

The charge distribution in solute electronic states can often depend markedly on the solvent. Thus in an electron donor-acceptor solute pair there is a competition between the electronic coupling V_{el}, which tends to delocalize the electron between the D and A sites, and the electrostatic interactions with the polar solvent, which tend to localize the electron on one of the sites. These aspects have been studied, particularly in a spectroscopic context, in early important work by several groups [31].

In all this work, however, it was assumed that the solvent was completely in equilibrium with the solute charge distribution. For charge transfer rate and relaxation problems, however, this equilibrium assumption perforce does not hold. Kim and Hynes have recently constructed a theoretical description for this nonequilibrium problem [32]. It is assumed that the solvent electronic polarization is equilibrated to the solute charge distribution, but that the solvent orientational polarization need not be. This leads to a nonlinear Schroedinger equation which is then solved to find the solute wave functions (and thus charge distributions) and the system free energies under nonequilibrium conditions.

Here we briefly describe just one result that emerges from this theory, for the activation free energy $\Delta G^{\ddagger}$ for electronically adiabatic ET reactions (Fig. 9). To place this in perspective,

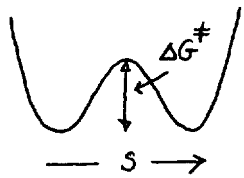

Figure 9. Schematic free energy curve for an adiabatic ET reaction indicating the activation free energy $\Delta G^{\ddagger}$. Here s denotes a solvent coordinate.

we first recall that the activation free energy for a symmetric charge shift $D^- + A \rightarrow D +$ harmonic A^- reaction is conventionally constructed [14] by finding the intersection of the two diabatic free energy curves for the localized reactant ($D^- + A$) and product ($D + A^-$) states, and then subtracting the electronic coupling V_{el}. This gives, for a dielectric continuum solvent model, the standard and widely employed result

$$\Delta G^{\ddagger} = \frac{e^2}{4}\left(\frac{1}{\varepsilon_\infty} - \frac{1}{\varepsilon_0}\right)\left(\frac{1}{2R_D} + \frac{1}{2R_A} - \frac{1}{R_{AD}}\right) - V_{el} \ , \tag{13}$$

where the R's are radii and R_{AD} is the AD separation, and ε_∞ and ε_0 are the high frequency and static dielectric constants. By contrast, the Kim-Hynes theory gives the approximate result

$$\Delta G^{\ddagger} = \frac{e^2}{4}\left(1 - \frac{1}{\varepsilon_0}\right)\left(\frac{1}{2R_D} + \frac{1}{2R_A} - \frac{1}{R_{AD}}\right) - V_{el} \ . \tag{14}$$

The origin of the difference in Eqs. (13) and (14) is the following [32]. In Eq. (13), the factor $(\varepsilon_\infty^{-1} - \varepsilon_0^{-1})$ represents the feature that the orientational polarization is fixed in the ET act, while the solvent electronic polarization keeps up. But, it is critical to note, the electronic polarization is that appropriate to the charge localized, nonadiabatic states. Eq. (14) instead refers to a transition state with a fixed orientational polarization, but with a solvent electronic polarization which is equilibrated to an adiabatic, charge delocalized symmetric transition state. In fact, the first term in Eq. (14) is essentially the difference in the equilibrium solvation free energies of the delocalized symmetric transition state and the localized reactant state [32]; this is reflected in the appearance of the $(1 - \varepsilon_0^{-1})^{-1}$ factor. Since in highly polar solvents $\varepsilon_0 >> \varepsilon_\infty \approx 2$, there is roughly a factor of two difference in the predictions of Eqs. (13) and (14), which is a very large effect for the ET rate constant, which depends exponentially on $\Delta G^{\ddagger}$. It is clearly of considerable interest to assess the validity of Eq. (14) compared to Eq. (13).

The interplay between the solute quantum charge distribution and the solvent electronic and orientational polarization should prove to be quite important in the understanding of a wide array of dynamic spectroscopic and kinetic problems involving charge transfer.

ACKNOWLEDGMENTS

This work was supported in part by NSF grants CHE84-19830 and CHE88-07852 (JTH), the Natural Sciences and Engineering Research Council of Canada (RK), the donors of the Petroleum Research Fund, administered by the American Chemical Society (JTH, RK), EEC Contract No. ST2J-0094 (GC) and a NATO International Collaborative Grant. We acknowledge the Italian CNR for the allocation of computer time via the CRAY project on Statistical Mechanics, and through the P.F. "Sistemi Informatici Calcolo Parallelo", a grant from the Pittsburgh Supercomputer Center (JTH), and the Research Board of the University of Toronto and the Ontario Center for Large Scale Computation for grants of CRAY computer time. We thank Dr. M. Newton for suggesting the use of the adiabatic Hamiltonian Eq. (7). The work described in Sec. 3 commenced during a series of CECAM workshops in Orsay (1986-88), and we thank the other members of the workshops for useful discussions and Dr. C. Moser for his support and hospitality.

REFERENCES

1. For a recent review, see R. A. Friesner and Y. Won, submitted to *Biochim. Biophys. Acta.*

2. See, e.g., M. A. Kahlow, W. Jarzeba, T. J. Kang and P. F. Barbara, *J. Chem. Phys. 90*, 151(1989) and references therein, particularly to the work of the Fleming and Simon groups.

3. B. Bagchi, D. W. Oxtoby and G. R. Fleming, *Chem. Phys. 86*, 259(1984); G. van der Zwan and J. T. Hynes, J. Phys. Chem. *89*, 4181(1985).

4. D. A. Karim, D. J. Haymet, M. Banet and J. D. Simon, *J. Phys. Chem. 92*, 3391(1988); M. P. Maroncelli and G. R. Fleming, *J. Chem. Phys. 89*, 5044(1988); J. S. Bader and D. Chandler, *Chem. Phys. Let. 157*, 501(1989).

5. E. A. Carter and J. T. Hynes, submitted to *J. Chem. Phys.*

6. G. Ciccotti, M. Ferrario, J. T. Hynes and R. Kapral, *Chem. Phys. 129*, 241(1989).

7. S. Nose, *J. Chem. Phys. 81*, 511(1984).

8. L. Verlet, *Phys. Rev. 159*, 98(1967).

9. See, e.g., J. P. Hansen, in *Molecular Dynamics Simulation of Statistical Mechanical Systems*, G. Ciccotti and W. Hoover, Eds. (North Holland, New York, 1986).

10. G. Ciccotti and J. P. Ryckaert, *Comput. Phys. Rep. 4*, 345(1986).

11. D. A. Zichi, H. J. Kim, E. A. Carter and J. T. Hynes, submitted to *J. Chem. Phys.*

12. E. A. Carter and J. T. Hynes, *J. Phys. Chem. 93*, 2184(1989).

13. See, e.g., B. J. Gertner, K. R. Wilson and J. T. Hynes, *J. Chem. Phys. 90*, 3537(1989) and references therein.

14. R. A. Marcus, *J. Chem. Phys. 24*, 966, 979(1956); M. D. Newton and N. Sutin, *Ann. Rev. Phys. Chem. 35*, 437(1984).

15. L. D. Zusman, *Chem. Phys. 49*, 295(1980).

16. D. F. Calef and P. G. Wolynes, *J. Phys. Chem. 87*, 3387(1983); H. L. Friedman and M. D. Newton, *Faraday Discuss. Chem. Soc. 74*, 73(1982); H. Sumi and R. A. Marcus, *J. Chem. Phys. 84*, 4272(1986); I. Rips and J. Jortner, *J. Chem. Phys. 87*, 2090(1987).

17. J. T. Hynes, *J. Phys. Chem. 90*, 3701(1986).

18. See, e.g., G. E. McManis and M. J. Weaver, *J. Chem. Phys. 90*, 912(1989); S. G. Su and J. D. Simon, *J. Chem. Phys. 89*, 908(1988).

19. D. A. Zichi, G. Ciccotti, M. Ferrario and J. T. Hynes, *J. Phys. Chem*, in press.

20. For other simulation studies of different aspects of ET reactions, see e.g., J K. Hwang and A. Warshel, *J. Am. Chem. Soc., 109*, 715(1987); R. A. Kuharski, J. S. Bader, D. Chandler, M. Sprik, M. L. Klein and R. W. Impey, *J. Chem. Phys. 89*, 3248(1988); J. W. Halley and J. Hautman, *Phys. Rev. B, 38*, 11704(1988); C. Zheng, J. A. McCammon and P. G. Wolynes, 1989 preprint.

21. A. Warshel, *J. Phys. Chem. 86*, 2218(1982).

22. T. Yamamoto, *J. Chem. Phys. 33*, 281(1960).

23. R. Kapral, *J. Chem. Phys. 56*, 1842(1972).

24. D. Chandler, *J. Chem. Phys. 68*, 2959(1978).

25. S. H. Northrup and J. T. Hynes, *J. Chem. Phys. 73*, 2715(1980).

26. R. O. Rosenberg, Jr., B. J. Berne, and D. Chandler, *Chem. Phys. 75,* 162(1980); J. S. Montgomery, Jr., D. Chandler and B. J. Berne, *J. Chem. Phys. 70,* 4056(1979).

27. J. P. Bergsma, B. J. Gertner, K. R. Wilson and J. T. Hynes, *J. Chem. Phys. 86,* 1356(1987); J. P. Bergsma, J. R. Reimers, K. R. Wilson and J. T. Hynes, *J. Chem. Phys. 85,* 5625(1986).

28. E. A. Carter, G. Ciccotti, J. T. Hynes and R. Kapral, *Chem. Phys. Lett. 156,* 472(1989).

29. G. Ciccotti, M. Ferrario, J. T. Hynes and R. Kapral, submitted to *J. Chem. Phys.*

30. R. F. Grote and J. T. Hynes, *J. Chem. Phys. 73,* 2715(1980); J. T. Hynes, in *The Theory of Chemical Reaction Dyanmics,* M. Baer, Ed. (CRC, Boca Raton, FL, 1985). Vol. IV, p. 171.

31. See, e.g., H. Beens and A. Weller, *Chem. Phys. Lett. 3,* 666(1969); S. Yomosa, *J. Phys. Soc. Jpn. 35,* 1738(1973); *44,* 602(1978); N. Mataga and T. Kubota, *Molecular Interactions and Electronic Spectra,* (M. Dekker, New York, 1970).

32. H. J. Kim and J. T. Hynes, to be submitted.